DOI 10.5012/bkcs.2011.32.1.196

Influence of Aminized Graphite Nanosheets on the Physical Properties of PMMA-based Nanocomposites

Ki-Seok Kim and Soo-Jin Park*

*Department of Chemistry, Inha University, Incheon 402-751, Korea. *E-mail: sjpark@inha.ac.kr*
Received June 12, 2010, Accepted November 12, 2010

In this work, poly(methyl methacrylate) (PMMA) was grafted onto amine treated graphite nanosheets (NH_2-GNs) and the surface characteristics and physical properties of the NH_2-GNs-g-PMMA films were investigated. The graft reaction of NH_2-GNs and PMMA was confirmed from the shift of the N_{1S} peak, including amine oxygen and amide oxygen, by X-ray photoelectron spectroscopy (XPS). The surface characteristics of the NH_2-GNs-g-PMMA films were measured as a function of the NH_2-GN content using the contact angle method. It was revealed that the specific component of the surface free energy (γ_s) of the films was slightly increased as the NH_2-GN content increased. Also, the thermal and mechanical properties of the NH_2-GNs-g-PMMA films were enhanced with the addition of NH_2-GNs. This can be attributed to the chemical bonding caused by the graft reaction between the NH_2-GNs and the PMMA matrix.

Key Words: Composites, Interfaces, Surface properties, Electrical properties, Mechanical properties

Introduction

Polymer nanocomposites based on carbon materials are expected to replace the traditional materials used in the electronics industry. A considerable amount of research has been conducted that centers on this technology owing to the superior thermal, mechanical, and electrical properties it offers. It is also inexpensive and lightweight and is known for its flexible features and simple processing techniques.[1,2]

Among the many carbon materials, graphites are naturally abundant. They are widely used as conductive filler to obtain conductive polymer composites as they have an excellent conductivity rating of 10^4 S/cm.[3] Graphites are composed of carbon nanolayers which are bound by weaker van der Waals force. These characteristics of graphites result in the formation of the graphite intercalation compound (GIC), also known as graphite oxide (GO). Exploiting the rapid heating of GO has led to what is known as expanded graphites (EGs), which are characterized by their high aspect ratio and low density. Polymer nanocomposites based on EGs show higher thermal, mechanical, and electrical properties with a low EG content compared to conventional carbon fillers.[4-6]

More recently, in an effort to improve the properties of the polymer nanocomposites with less filler content, graphite nanosheets (GNs) have received much attention as a type of nanoscale filler. GNs are easily prepared by exfoliation of EGs *via* ultrasonic treatment. They have a high dispersity rating and a high aspect ratio, leading to nanocomposites with superior thermal, physical, and electrical properties.[7,8] However, these properties are strongly dependent on the dispersity and interaction of the carbon fillers in the polymer matrix, as these carbon fillers are non-uniformly dispersed in the polymer matrix due to the van der Waals interaction between them. Therefore, in an effort to alleviate this non-uniformity, various methods have been utilized with these nanocomposites, including surface functionalization, *in-situ* polymerization, and ultrasonication, *etc*.[9-11]

Among the various polymers, poly(methylmethacrylate) (PMMA) is one of the most widely used thermoplastic due to its many excellent physical and optical properties. It can be simply prepared in many forms, such as fibers, films, and moldings with various fillers. This makes it viable for use in a range of applications, including glazing, lighting, architecture, transportation, and bio materials.[12-14]

Therefore, in this work, GNs as conductive fillers are functionalized by ethylenediamine, and poly(methylmethacrylate) (PMMA) is then grafted onto amine-treated GNs (NH_2-GNs). NH_2-GNs-g-PMMA films are prepared in a solution casting method after a graft reaction. The surface characteristics and physical properties of the NH_2-GNs-g-PMMA films are investigated.

Experimental

Materials. PMMA was obtained from LG MMA. The natural graphites (N-GP) were supplied from Aldrich. Thionyl chloride, tetrahydrofuran (THF), chloroform, and ethylenediamine (EDA) were supplied from Aldrich.

Preparation of Amine Treated GNs. EGs were produced by chemical oxidation using a sulfuric and nitric acid solution in conjunction with a rapid heat treatment at a temperature of 1000 °C for 90 s. GNs were obtained by exfoliation of the EGs *via* an ultrasonic treatment for 6 h in acetone.

For the surface treatment of the GNs, they were further acid-reacted with a sulfuric acid and nitric acid (3:1) mixture that was stirred for 3 h. They were then washed and dried at 80 °C. In the next step, the dried GNs were put in an excess amount of thionyl chloride and the mixture was stirred at 70 °C for 24 h. The excess thionyl chloride was decanted and the acyl-derivated GNs (GNs-COCl) were washed by THF and dried under a vacuum at room temperature. Finally, the GNs-COCl was reacted with excess EDA at 100 °C for 12 h and then washed by THF and dried at 80 °C. It was termed NH_2-GNs.

Preparation of NH_2-GNs-g-PMMA Films. The NH_2-GNs-g-PMMA films were prepared with different NH_2-GN contents

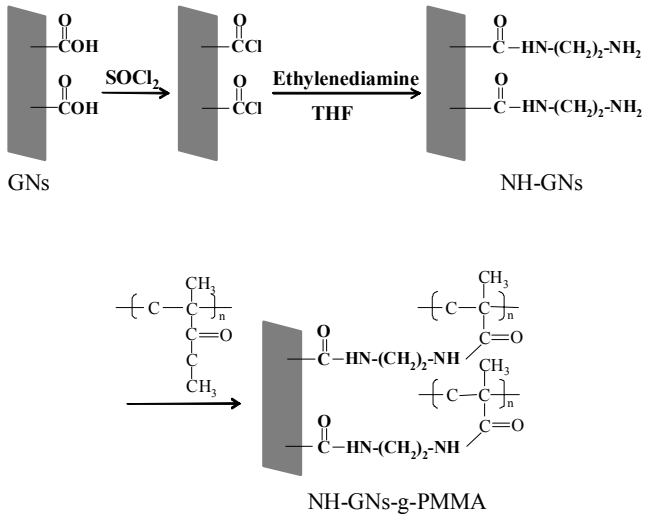

Figure 1. Schematic diagram showing the preparation of the NH_2-GNs and NH_2-GNs-g-PMMA.

using a solution blending method. The NH_2-GNs concentrations were 1, 2, 3, and 4 wt % of the total PMMA weight. In this process, PMMA was dissolved in chloroform and NH_2-GNs were then dispersed in PMMA solution with sonication for 3 h. Finally, the NH_2-GNs and PMMA were reacted for 12 h at 70 °C while stirring. NH_2-GNs-g-PMMA films were prepared in a solution casting method and were then dried in an oven at 80 °C. The product was then dried in a vacuum oven at 80 °C for 2 days. The preparation procedure of the NH_2-GNs and NH_2-GNs-g-PMMA is presented in Fig. 1.

Measurements. The surface morphologies of NH_2-GNs and NH_2-GNs-g-PMMA films were observed by scanning electron microscopy (SEM, S-4200, Hitachi) and transmission electron microscopy (TEM, Jeol FE-TEM 2006).

The structures of the pure PMMA and NH_2-GNs-g-PMMA film were determined by X-ray diffraction (XRD, Rigaku D/Max 2200 V) at 40 kv and 40 mA using Cu Kα radiation. The XRD patterns were obtained in 2θ ranges between 2° and 70° at a scanning rate of 2°/min.

NH_2-GNs and NH_2-GNs-g-PMMA films were characterized by X-ray photoelectron spectroscopy (XPS, K-Alpha) using a VG Scientific ESCALAB MK-II spectrometer equipped with an Mg Kα (1253.6 eV) X-ray source, a high-performance multichannel detector that was operated at 200 W.

Contact angles were measured using the sessile drop method on a Rame-Hart goniometer. Approximately 5 μL of wetting liquid was used for each measurement at a temperature of 20 °C. A reading within 5 s of the formation of a drop was taken for the critical surface tension measure. The testing liquids used were deionized water, diiodimethane, and ethylene glycol. The basic characteristics of the surface free energy of the liquids are given in Table 1.

Table 1. Surface free energy and related components of the liquids, measured at 20 °C (mJ/m^2)

	γ_L	γ_L^L	γ_L^{SP}	γ_L^+	γ_L^-
Water	72.8	21.8	51.0	25.5	25.5
Diiodomethane	50.8	50.42	0.38	0	0
Ethylene glycol	47.7	31.0	16.7	1.92	47.0

The electrical conductivity of the NH_2-GNs-g-PMMA films was measured at room temperature using a four-probe digital multimeter (MCP-T610, Mitsubishi Chem.).

The thermal stability of the NH_2-GNs-g-PMMA films was measured by means of thermogravimetric analyses (TGA, DuPont TGA-2950 analyzer) from 30 to 850 °C at a heating rate of 10 °C/min in a nitrogen atmosphere.

The mechanical properties of the NH_2-GNs-g-PMMA films were measured using the tensile strength method on a universal testing machine (UTM, Lloyd, LR5K). Each sample was tested at a crosshead speed of 2 mm/min at room temperature.

Results and Discussion

Characterization of NH_2-GNs. Fig. 2 shows NH_2-GNs images after the ultrasonic and surface treatment. After powdering the EGs, the worm-like EGs were exfoliated by the ultrasonic treatment, producing a thin plate form with a dimension from a few μm to nearly 18 μm and a nano-size thickness. It was clear that the NH_2-GNs had a high aspect ratio. The thin-plate-type NH_2-GNs were further observed *via* TEM, as shown in Figs. 2 (b) and (c).

Fig. 3 presents TGA thermograms of the N-GP, GNs, and NH_2-GNs. As shown in Fig. 3, N-GP shows high thermal stability up to 800 °C. However, the GNs and NH_2-GNs show the two weight loss intervals. GNs show a low weight loss from 180 to 660 °C due to the decomposition of the organic functional groups of the carboxyl and hydroxyl groups which formed during the preparation of GNs. They also show a sharp inflection peak at 660 °C, which can be attributed to the thermal decomposition of GNs. The NH_2-GNs show additional weight loss from 130 to 660 °C compared to the GNs. The greater weight loss at a low temperature most likely resulted from the increased thermal decomposition of organic functional groups containing carboxyl, hydroxyl, and amine groups on the GNs due to the additional chemical treatment.

Grafting of PMMA onto NH_2-GNs. Fig. 4 shows XRD pa-

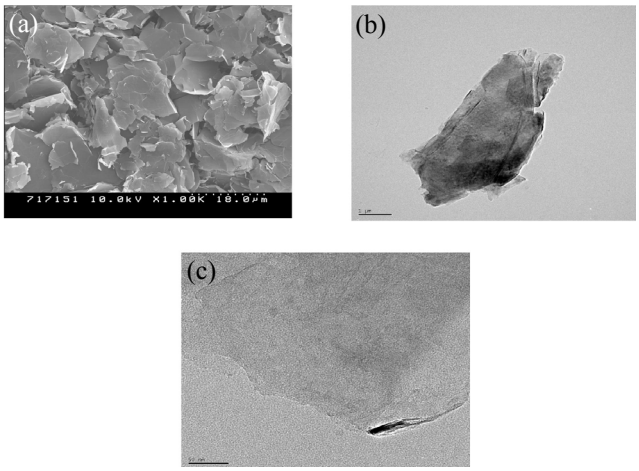

Figure 2. SEM (a) and TEM (b, c) images of NH_2-GNs.

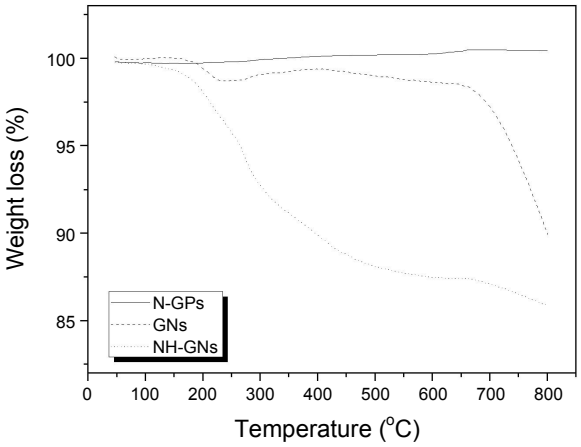

Figure 3. TGA thermograms of N-GPs, GNs, and NH_2-GNs.

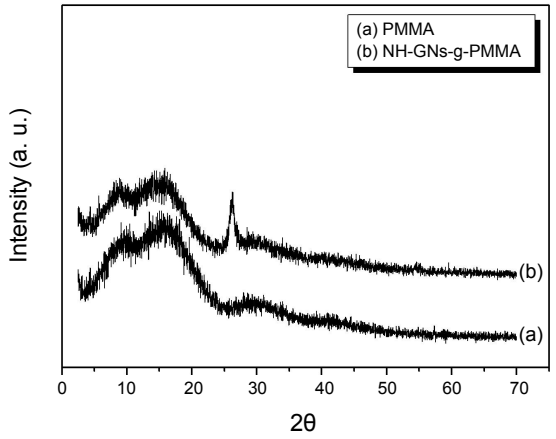

Figure 4. XRD patterns of pure PMMA and NH_2-GNs-g-PMMA films.

tterns of the pure PMMA and NH_2-GNs-g-PMMA films. As expected, the NH_2-GNs-g-PMMA film shows a weak graphite diffraction (002) peak at approximately $2\theta = 26^o$, whereas the pure PMMA film is amorphous. This indicates that the NH_2-GNs are randomly oriented in the PMMA matrix, resulting in a decrease in the number of regular planes that satisfy the Bragg's equation at $2\theta = 26^o$.

The grafting of PMMA onto the NH_2-GNs is confirmed by XPS analysis, as shown in Fig. 5. The N_{1S} peak of the NH_2-GNs can be curve-fitted with three component peaks, as shown in Fig. 5 (a). The lower binding energy peak at 398.7 eV is attributed to the amine nitrogen. The higher binding energy peaks at 400.0 and 401.5 eV are attributed to the amide nitrogen by the electron-withdrawing carbonyl group. Fig. 5 (b) shows the N_{1S} spectrum of the NH_2-GNs-g-PMMA films after the graft reaction. The N_{1S} peak can also be curve-fitted with two component peaks, one at 400.0 eV and one at 401.5 eV. The absence of the amine nitrogen peak at 398.7 eV reveals that all of the amine groups of the NH_2-GNs have reacted with the PMMA.

In Fig. 5 (c), the O_{1S} peak of pure PMMA can be curve-fitted with two component peaks. The peaks at 532.7 eV and 533.8 eV arise from carbonyl oxygen and ether oxygen, respectively. The O_{1S} peak of the NH_2-GNs-g-PMMA films can be also curve-fitted with two component peaks (amide oxygen and ether

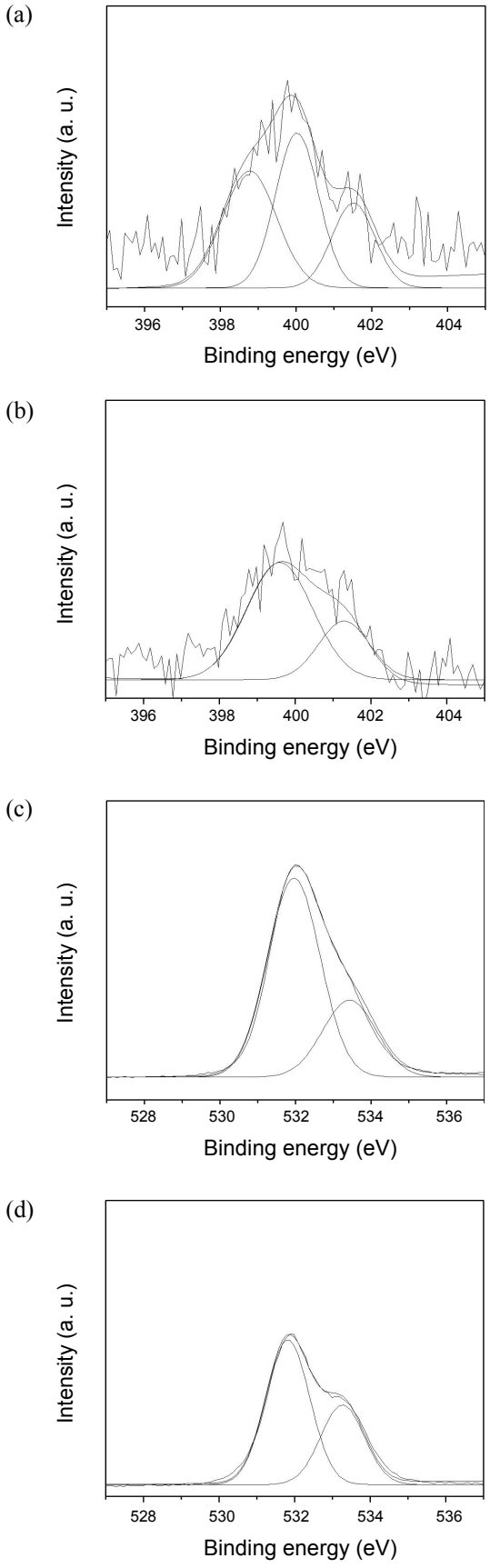

Figure 5. XPS N_{1S} spectra of NH_2-GNs (a), NH_2-GNs-g-PMMA films (b) and O_{1S} spectra of pure PMMA (c), NH_2-GNs-g-PMMA films (d).

oxygen); is the peaks are broader and the intensity of the amide oxygen peak is lower as compared with the pure PMMA. This is clearly attributable to the decrease of the amide oxygen due to the grafting reaction of the NH_2-GNs and PMMA.

Surface Energetics of the Films. The measurement of the contact angle is a well known as useful technique to investigate the characteristics of a surface using polar liquids and nonpolar liquids, the hydrophilic-hydrophobic property, acid-base interactions, and the van der Waals force. The London dispersive and specific components, including the electron acceptor and donor parameters of the surface free energy of the films, were determined by measuring the contact angles of three testing liquids with known London dispersive and specific components. The surface free energy of the films was calculated according to the following equation, as proposed by Owens and Wendt[15] and Kaelble,[16] using the geometric mean:

$$\gamma_L(1+\cos\theta) = 2(\gamma_L^L\gamma_S^L)^{1/2} + 2(\gamma_L^{SP}\gamma_S^{SP})^{1/2} \quad (1)$$

Here, the subscripts L and S represent the liquid and solid states, and γ^L and γ^{SP} are the London dispersive (superscript: L) and specific (superscript: SP, Debye, Keesom of the van der Waals force, H-bonding, π-bonding, and other small polar effects) components of the surface free energy of the constitutive elements, respectively.

Table 2 summarizes the calculated results of the surface free energy and their components for the pure PMMA and NH_2-GNs-g-PMMA films investigated in terms of their contact angles. The surface free energy of the films decreased as the NH_2-GN content increased, mainly due to the decrease of the London dispersive component. In contrast, the specific component increased slightly, resulting from the polar group increase of the GNs caused by the chemical treatment. These results suggest that the NH_2-GNs do not significantly affect the surface characteristics of the films due to an addition of a relatively low NH_2-GN content.

Electrical Properties of the Films. The electrical conductivity of the NH_2-GNs-g-PMMA films was measured using a four-probe method. The electrical conductivity of the films was examined as a function of the NH_2-GN content. This is listed in Table 3. Generally, graphite nanoplate filler provide higher improvement of the thermal and electrical conductivity compared with carbon nanotubes, wihic is attributed to the strong interaction between graphite nanoplate of flate type and polymer matrix and high aspect ratio of graphite nanoplates.[17] The findings show that the electrical conductivity of the pure PMMA film is not detectable (over the limit of the equipment). However, the electrical conductivity of the films increases remarkably with an increase of the NH_2-GN content. It was found that the increase in the NH_2-GN content causes the formation of a conductive network, resulting in additional conductive pathways.[18]

Fig. 6 shows the surface of the NH_2-GNs-g-PMMA film as a function of the NH_2-GN content. In PMMA films containing 1 wt % NH_2-GNs, the NH_2-GNs are well dispersed in the PMMA matrix, whereas NH_2-GNs become aggregated as the NH_2-GN content increases. This suggests that aggregation between NH_2-GNs, resulting in multiple conductive networks, can improve the electrical conductivity as compared to well-dispersed NH_2-GNs.

Thermal Properties of the Films. The thermal stabilities of pure PMMA and PMMA films containing 4 wt % NH_2-GNs are shown in Fig. 7. The initial decomposed temperature (IDT) of the NH_2-GNs-g-PMMA film is higher (299.8 °C) than that of the pure PMMA film (120.4 °C). The NH_2-GNs-g-PMMA films become degraded near 312 °C, which is higher compared to the degradation temperature of pure PMMA (270 °C). This

Table 2. Surface free energy and related components for pure PMMA and NH_2-GNs-g-PMMA films as a function of the NH_2-GN content, measured at 20 °C (mJ/m^2)

Sample	γ_S	γ_S^L	γ_S^{SP}
PMMA	40.66	40.45	0.21
NH_2-GNs-1	40.63	40.42	0.21
NH_2-GNs-2	40.49	40.19	0.30
NH_2-GNs-3	39.15	38.72	0.43
NH_2-GNs-4	38.76	38.21	0.55

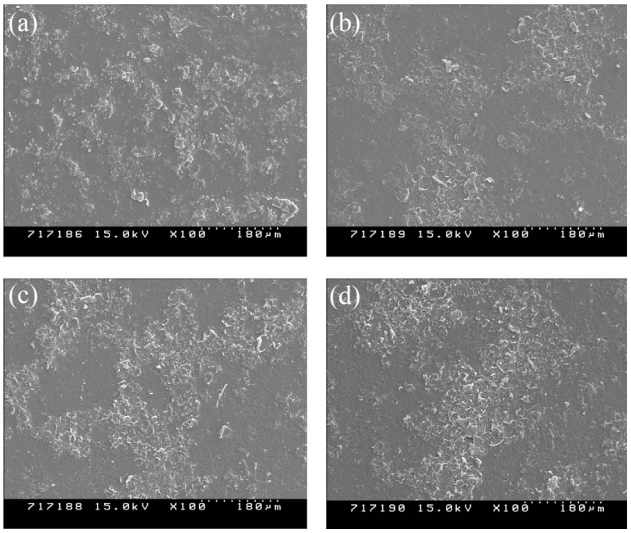

Figure 6. SEM images of NH_2-GNs-g-PMMA films as a function of the NH_2-GN content.

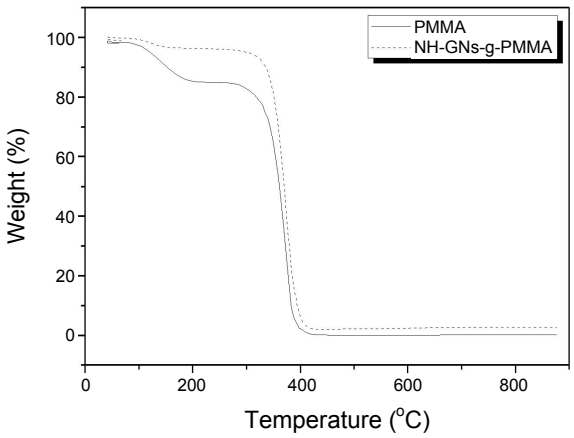

Figure 7. TGA thermogram of pure PMMA and 4 wt % NH_2-GNs-g-PMMA films.

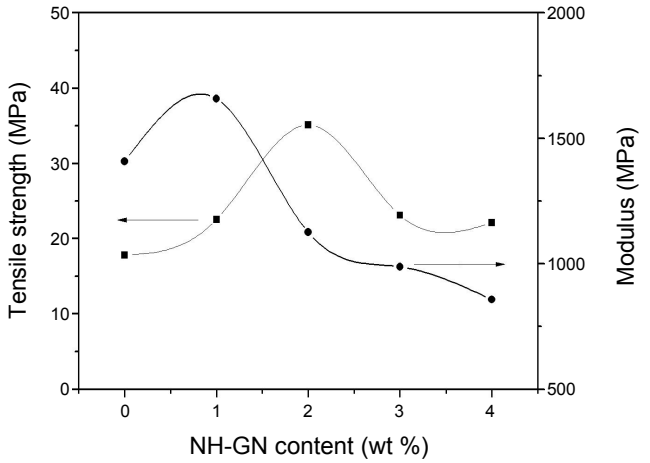

Figure 8. Tensile strengths and moduli of NH_2-GNs-g-PMMA films as a function of the NH_2-GN content.

Table 3. Electrical conductivity of NH_2-GNs-g-PMMA films as a function of the NH_2-GN content

NH_2-GNs (wt %)	Electrical conductivity (S/cm)
0	-
1.0	3.90×10^{-4}
2.0	2.01×10^{-2}
3.0	2.76×10^{-1}
4.0	5.20×10^{-1}

is attributed to the grafting between the NH_2-GNs and PMMA, which causes a trammel effect of the movement of the PMMA chains. In addition, no significant weight change was observed at temperatures in excess of approximately 450 ^{o}C; moreover, the residual weight percent is higher (2.8%) than that of the pure PMMA (0.3%). These results indicate that the difference in the total weight loss is most likely due to the excellent thermal stability of the NH_2-GNs dispersed in the PMMA matrix.[19,20]

Mechanical Properties of the Films. Fig. 8 shows the tensile strength and moduli of NH_2-GNs-g-PMMA films as a function of the NH_2-GN content. The tensile strength of the films is improved by the addition of NH_2-GNs. The maximum value is shown at 2 wt % NH_2-GNs, showing a value that exceeds approximately 97% as compared with the pure PMMA film. This is attributed to the chemical bonding caused by the graft reaction of the NH_2-GNs and the PMMA matrix. However, above 2 wt % NH_2-GN content, the tensile strength is decreased upon the accumulation of NH_2-GNs that occurs during the processing stage. The aggregates of NH_2-GNs result in weak interaction between the NH_2-GNs and the PMMA matrix. The moduli of the NH_2-GNs-g-PMMA films is also improved with the by nearly 17% compared with the pure PMMA film due to the better dispersion of NH_2-GNs in the PMMA matrix, leading to the strong interaction between the NH_2-GNs and the PMMA matrix.[21-24]

Conclusions

Amine-treated GNs-g-PMMA films were prepared by solution casting after a graft reaction. The grafting of PMMA onto the NH_2-GNs was confirmed by means of XPS, showing that it resulted from the shift of the N_{1S} peaks. The surface free energy of the film measured according to the contact angle was slightly decreased as the NH_2-GN content increased due to the decrease of the London dispersive component. The electrical conductivity of the NH_2-GNs-g-PMMA films increased as the NH_2-GN content increased due to the increase in the number of electron conductive pathways. Additionally, the thermal and mechanical properties of the NH_2-GNs-g-PMMA films were improved with the addition of NH_2-GNs. It was found that the NH_2-GNs were well dispersed in the PMMA matrix and that the grafting of NH_2-GNs and the PMMA matrix led to an effective reinforcement effect for the NH_2-GNs.

Acknowledgments. This paper was performed for the Carbon Dioxide Reduction and Sequestration R&D Center, one of the 21st Century Frontier R&D Program funded by the Ministry of Science and Technology of Korea.

References

1. Yasmin, A.; Luo, J. J.; Daniel, I. M. *Compos. Sci. Tech.* **2006**, *66*, 1182.
2. Kim, S.; Park, S. J. *Anal. Chimi. Acta* **2008**, *619*, 43.
3. Freris, I.; Cristofori, D.; Riello, P.; Benedetti, A. *J. Colloid Interface Sci.* **2009**, *331*, 351.
4. Toyoda, M.; Inagaki, M. *Carbon* **2000**, *38*, 199.
5. Hartono, T.; Wang, S.; Mab, Q.; Zhu, Z. *J. Colloid Interface Sci.* **2009**, *334*, 50.
6. Fawn, M. U.; Charles, A. W. *Polym. Degrad. Stab.* **2002**, *76*, 111.
7. Li, J.; Wong, P. S.; Kim, J. K. *Mater. Sci. Eng. A* **2008**, *483-484*, 660.
8. Kalaitzidou, K.; Fukushima, H.; Drzal, L. T. *Compos. Sci. Tech.* **2007**, *67*, 2045.
9. Chen, G.; Wu, C.; Weng, W.; Wu, D.; Yan, W. *Polymer* **2003**, *44*, 1781.
10. Choi, H. J.; Lim, J. Y.; Zhang, K. *Diamond Relate. Mater.* **2008**, *17*, 1498.
11. Yang, B. X.; Shi, J. H.; Pramoda, K. P.; Goh, S. H. *Compos. Sci. Tech.* **2008**, *68*, 2490.
12. Li, S.; Toprak, M. S.; Jo, Y. S.; Dobson, J.; Kim, D. K. *Adv. Mater.* **2007**, *19*, 4347.
13. Gross, S.; Camozzo, D.; Noto, V. D.; Armelao, L.; Tondello, E. *Euro. Polym. J.* **2007**, *43*, 4593.
14. Seo, M. K.; Park, S. J. *Mater. Sci. Eng. A* **2009**, *508*, 28.
15. Owens, D. K.; Wendt, R. C. *J. Appl. Polym. Sci.* **1969**, *13*, 1741.
16. Kaelble, D. H.; Uy, K. C. *J. Adhesion* **1970**, *2*, 50.
17. Yu, A.; Ramesh, P.; Itkis, M. E.; Bekyarova, E.; Haddon, R. C. *J. Phys. Chem. C* **2007**, *111*, 7565.
18. Martin, C. A.; Sandler, J. K. W.; Shaffer, M. S. P.; Schwarz, M. K.; Bauhofer, W.; Schulte, K.; Windle, A. H. *Compos. Sci. Tech.* **2004**, *64*, 2309.
19. Xiao, M.; Lu, Y.; Wang, S. J.; Zhao, Y. F.; Meng, Y. Z. *J. Power Sources* **2006**, *160*, 165.
20. Mo, Z.; Sun, Y.; Chen, H.; Zhang, P.; Zuo, D.; Liu, Y.; Li, H. *Polymer* **2005**, *46*, 12670.
21. Debelak, B.; Lafdi, K. *Carbon* **2007**, *45*, 1727.
22. Seo, M. K.; Lee, J. R.; Park, S. J. *Mater. Sci. Eng. A* **2005**, *404*, 79.
23. Kim, K. S.; Rhee, K. Y.; Lee, K. H.; Byun, J. H.; Park, S. J. *J. Ind. Eng. Chem.* **2010**, *16*, 572.
24. Zheming, G.; Chunzhong, L.; Gengchao, W.; Ling, Z.; Qilin, C.; Xiaohui, Li.; Wendong, W.; Shilei, J. *J. Ind. Eng. Chem.* **2010**, *16*, 10.